

Multifunctional biomimetic liposomal nucleic acid scavengers inhibit the growth and metastasis of breast cancer

Yuhang Miao, ‡^a Kaizhen Wang, ‡^a Xin Liu,^b Xin Wang,^a Yanwei Hu,^b Zhenwei Yuan,
^{ab} and Dawei Deng.^{ab}

^a Department of Pharmaceutical Engineering, and ^b Department of Biomedical Engineering, School
of Engineering, China Pharmaceutical University, Nanjing 211198, China.

E-mail: yuanzhenwei@cpu.edu.cn (Z. Yuan)

E-mail: dengdawei@cpu.edu.cn (D. Deng)

Synthesis of amphiphilic dendritic macromolecules

Amphiphilic dendritic macromolecules were synthesized using the amino esters method and subsequently modified. The initial reaction between t-butyl acrylate and propargyl amine was conducted in methanol as the solvent at room temperature for 72 hours. The resulting mixture was subjected to vacuum concentration and purified by column chromatography, yielding the first-generation dendritic molecule, designated as 1. Anhydrous dichloromethane (DCM) was employed as the solvent, and trifluoroacetic acid (TFA) was added dropwise under ice bath conditions. The reaction was stirred in the absence of light at room temperature for 72 hours and then concentrated under vacuum. Recrystallization from anhydrous ether produced a pale yellow solid, identified as 2. Solid 2 was dissolved in anhydrous dimethylformamide (DMF) under ice bath conditions, followed by gradual addition of chloroacetonitrile. The mixture was stirred at room temperature for 48 hours, then washed with distilled water and saturated salt water. Extraction with ethyl acetate (EA) and purification by column chromatography yielded a colorless oily compound, labeled as 3. Compound 3 was added dropwise under ice bath conditions to a reaction vessel, and after stirring at ambient temperature for 48 hours, the solvent was evaporated, resulting in a pale yellow oily compound, designated as 4. The synthesis of the final compound involved the reaction between compounds 3 and 4 under anhydrous conditions with ice protection and nitrogen atmosphere. Catalyzed by 1,8-diazabicyclo[5.4.0]undec-7-ene (DBU), the reaction was stirred at room temperature for 48 hours. The mixture was then concentrated, and the EA extract was washed with distilled water and saturated salt water. The product was reacted with benzoic anhydride at room temperature in the presence of 4-(Dimethylamino)pyridine (DMAP) as a catalyst for 3 hours. The mixture was washed with saturated NaHCO₃ solution and saturated NaCl. The crude product was purified by column chromatography. Compound 5 was dissolved in anhydrous DCM and stirred at room temperature with TFA for 48 hours. The product was crystallized using anhydrous ether, resulting in a white solid, denoted as 6. Under ice bath conditions, 6 was dissolved in DMF, and NEt₃ was added, followed by chloroacetonitrile. The mixture was stirred at 30°C for 36 hours. After solvent

evaporation, the reaction mixture was washed with distilled water and saturated NaCl, followed by extraction with EA. The crude product was purified by column chromatography, yielding a colorless oily substance, designated as 7. Compound 7 and N-Boc ethanolamine were dissolved in anhydrous acetonitrile (MeCN) under a nitrogen atmosphere, and DBU was added gradually at room temperature. The reaction mixture was stirred at 30°C for 12 hours. After solvent evaporation, the substance was washed with distilled water and saturated NaCl. The mixture was then extracted with DCM, and the crude product was purified by column chromatography to yield a colorless oily substance, denoted as 8.

For the end alkyl chain synthesis, 2 g of acid, 840 mg of 3,5-dihydroxybenzoate ester, and 500 mg of ethanol were used. The esterification reaction was catalyzed by EDC (430 mg) and DMAP (80 mg) and conducted at ambient temperature in anhydrous DCM for 24 hours. The reaction mixture was purified by column chromatography. The final amphiphilic dendritic macromolecules were synthesized through a copper-catalyzed azide-alkyne cycloaddition (CuAAC) click reaction at the hydrophilic and hydrophobic termini.

Bioavailability experiment

Iv administration to three rats, the drug dose was 1 mg/kg, and Po administration to three rats, the drug dose was 10 mg/kg. The rats were fasted for 12 h before administration and had free access to water during the experiment. 0.25, 0.5, 1, 2, 4, 8 and 24 hours after administration, 0.2 mL of blood was taken through the eye orbit and placed in an anticoagulation tube for later use. The required series of concentrations of the working solution were achieved by diluting the stock solution of the analyte with DMSO solution. 2 µL of the working solution (20, 50, 100, 200, 500, 1000, 2500, 5000, 10000, 40000 ng/mL) was added to 20 µL of blank mouse plasma to achieve a calibration standard of 2 to 4000 ng/mL (2, 5, 10, 20, 50, 100, 250, 500, 1000, 4000 ng/mL) in 22 µL. Four plasma quality control samples were prepared at concentrations of 2 ng/mL, 5 ng/mL, 50 ng/mL and 2000 ng/mL. These quality control samples were prepared on the day of analysis in the same way as the calibration standards. 22 µL of the standard, 22 µL of the control sample and 22 µL of the unknown sample (20 µL

mouse plasma containing 2 μ L blank solution) were added to 80 μ L of the IS mixture containing acetonitrile for protein precipitation. The samples were then vortexed for 30 seconds. After centrifugation at 12,000 rpm at 4 °C for 10 minutes, the supernatant was diluted 1-fold with water. 2 μ L of the diluted supernatant was injected into the LC/MS/MS system for quantitative analysis.

Western blot assay

Western blot analysis was performed according to standard protocols. MDA-MB-231 and MCF-7 cells were washed twice with cold PBS, and total protein was extracted using pre-chilled lysis buffer. The protein samples were separated by SDS-PAGE and transferred to polyvinylidene fluoride (PVDF) membranes (Bio-Rad, CA, USA). After transfer, the membranes were incubated with specific primary antibodies: active Caspase 3 (Abcam, ab32042), Caspase 3 (Abcam, ab32351), Bax (Abcam, ab32503), Bcl-2 (Abcam, ab182858), GAPDH (Cell Signaling Technology, 97166), E-Cadherin (Cell Signaling Technology, 3195), N-Cadherin (Cell Signaling Technology, 13116), Snail (Cell Signaling Technology, 3879), Vimentin (Cell Signaling Technology, 5741), TLR-9 (Abcam, ab134368), MyD88 (Abcam, ab133739), P-NF- κ B p65 (Abcam, ab76302), NF- κ B p65 (Abcam, ab32536), and β -Actin (Abcam, ab6276). Immunocomplexes were visualized using chemiluminescence with ECL reagents (Vazyme, China) and quantified using ImageJ software.

RNA extraction and quantitative RT-PCR

Total RNA was extracted using an RNA extraction kit (Yishan, Shanghai, China) following the manufacturer's instructions. cfDNA was synthesized using a HiScript Q RT SuperMix kit (Vazyme, China). cfDNA was analyzed by quantitative RT-PCR on a LightCycler 480 Real-Time Fluorescent Quantitative PCR System (Roche, Germany). All qPCR amplifications were conducted in triplicate and repeated across three independent experiments. The qPCR primer sequences are detailed in Table S1.

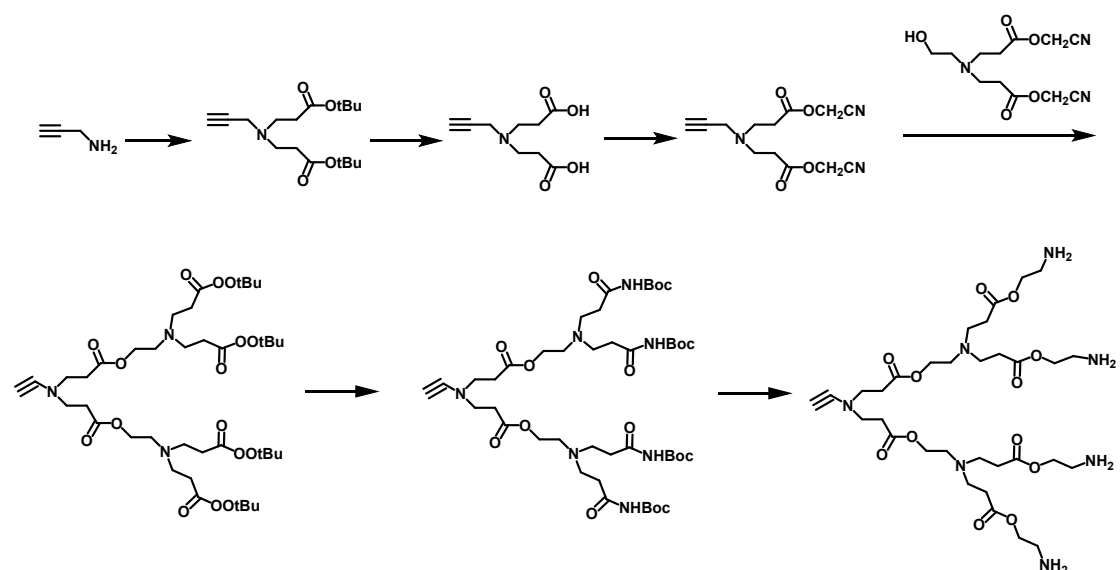


Figure S1. Synthesis route of hydrophilic end of amphiphilic dendritic macromolecules.

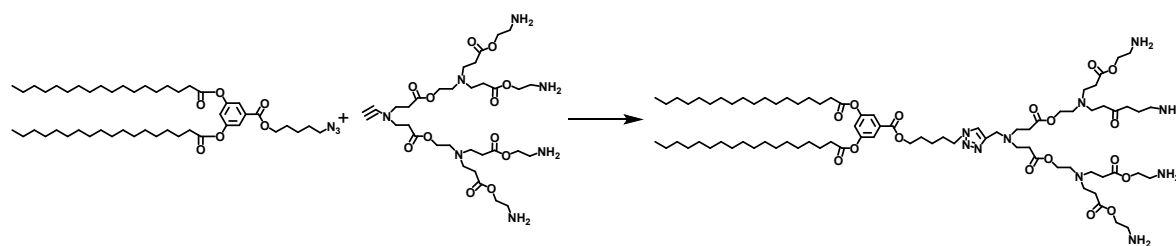


Figure S2. The synthesis route of amphiphilic dendritic macromolecules.

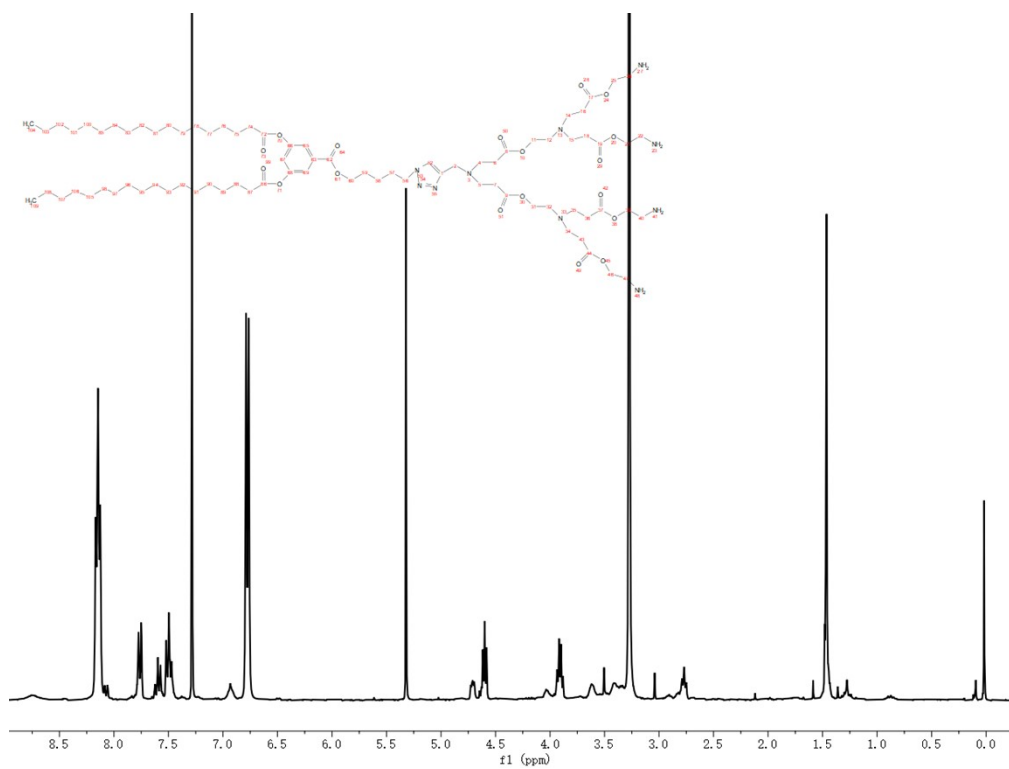


Figure S3. ¹H NMR spectrum of dendritic monomers.

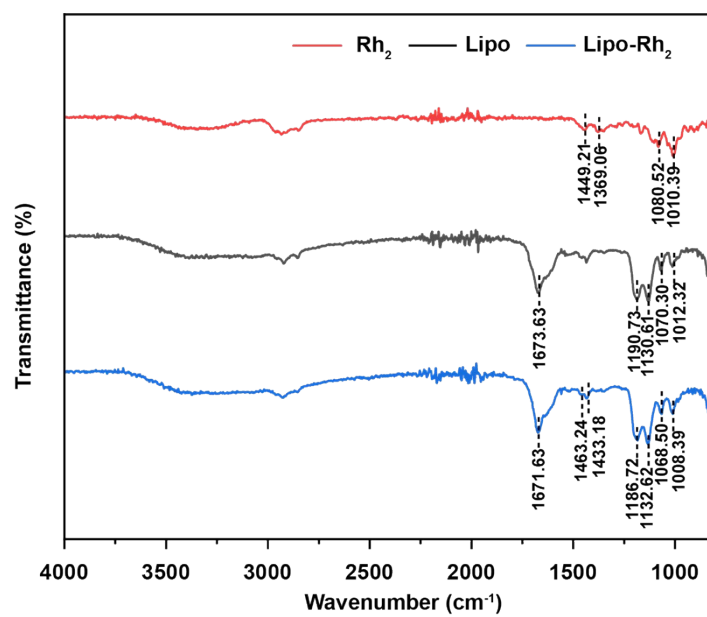


Figure S4. Fourier transform infrared spectra of Lipo, Rh₂ and Lipo-Rh₂.

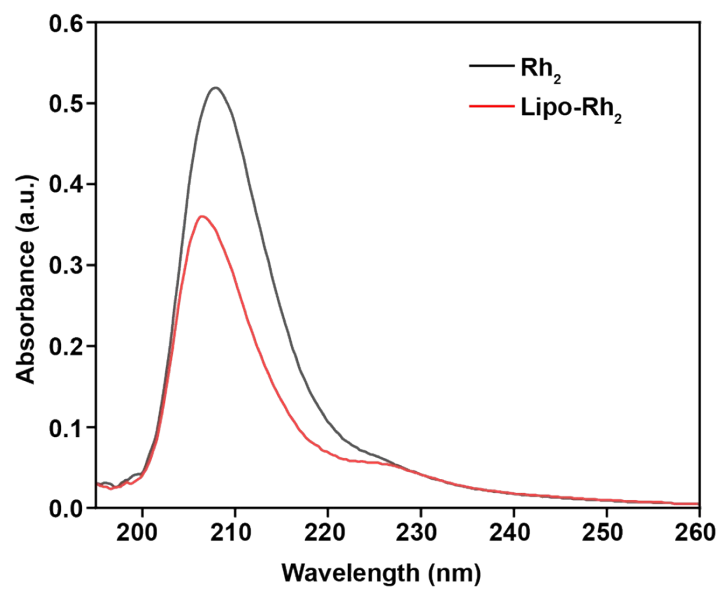


Figure S5. Ultraviolet spectra of Rh₂ and Lipo-Rh₂.

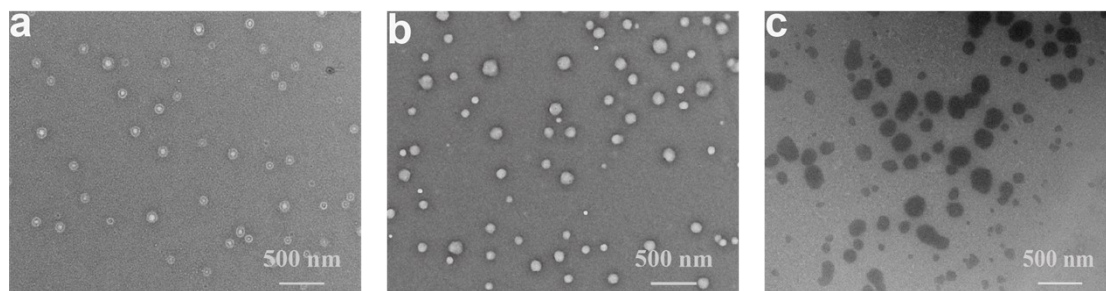


Figure S6. (a) TEM image of amphiphilic dendritic macromolecules self-assembling into a bilayer structure. (b) TEM image of cholesterol embedded in amphiphilic dendritic macromolecules. TEM images of Rh₂ embedded in amphiphilic dendritic macromolecules.

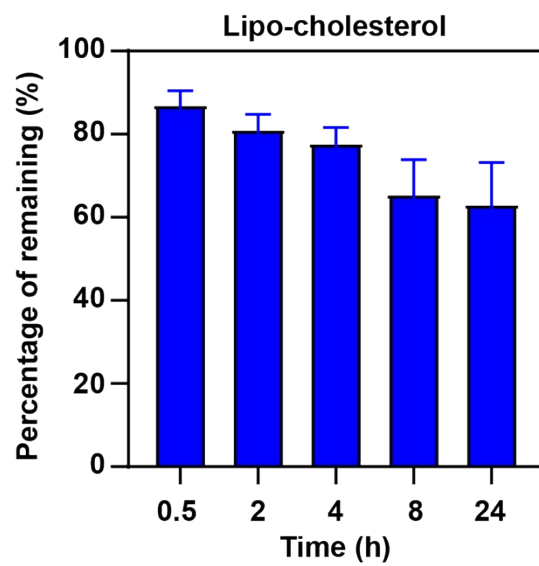


Figure S7. The in vitro stability of Lipo-cholesterol in the plasma of SD rats was 0.5-24 hours (n = 3).

The simulated system comprised a bilayer membrane containing 200 amphiphilic dendrimer-like macromolecules, evenly distributed with 100 molecules per layer. The system included 46,864 water molecules and was periodic, with an initial box size of $19 \times 19 \times 16 \text{ nm}^3$. Molecular dynamics simulations were performed using GROMACS 2018.6, with visualization primarily conducted using VMD software and data processing for images carried out with Xmgrace. The TIP3P model was employed for water representation. The simulation was executed in the NPT ensemble, with temperature controlled at 310 K using a Nose-Hoover thermostat and pressure maintained at 1 bar using the Parrinello-Rahman method. The LINCS algorithm was applied to constrain all bonds, and the particle-mesh Ewald (PME) algorithm was used for electrostatic interactions. Van der Waals interactions were computed with a cutoff distance of 12 Å. A 100-nanosecond dynamic simulation was conducted, with coordinates saved at 2-picosecond intervals for subsequent analysis.

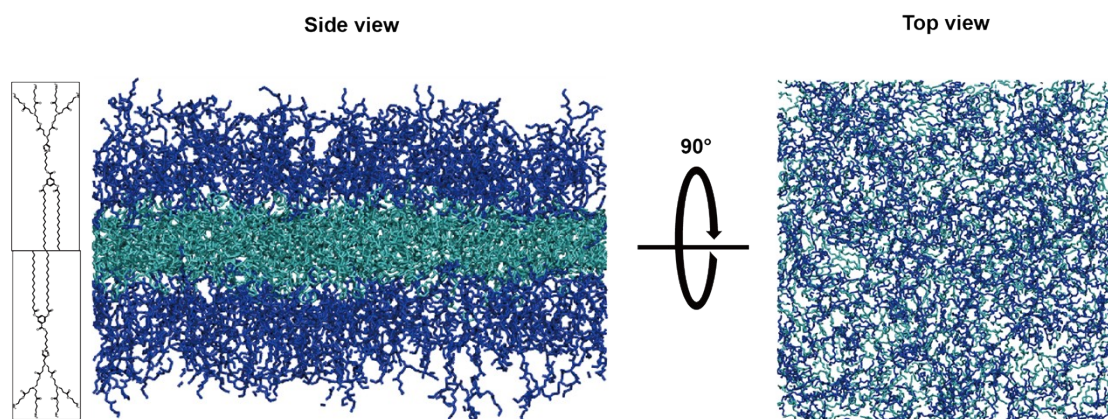


Figure S8. Build a tree-like structure of large molecular monolayer membrane.

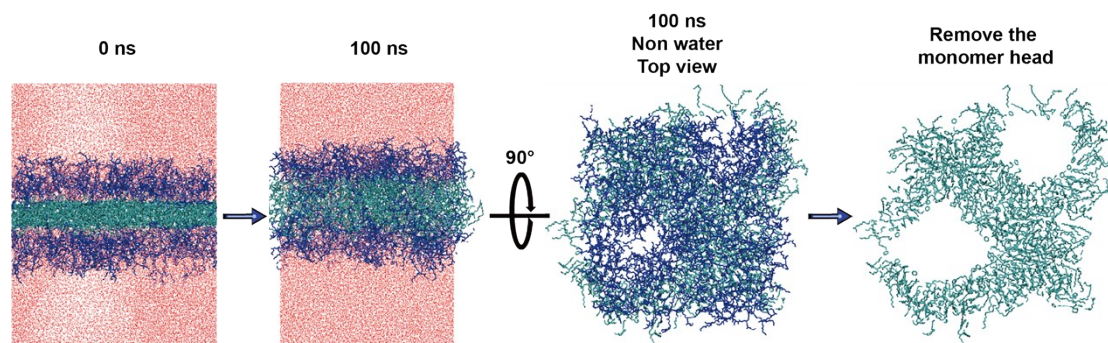


Figure S9. After 100 nanoseconds, the monomers of the dendritic macromolecule spontaneously assembled into a ring structure, with a hydrophilic head (depicted in blue in the diagram) on the outer layer and a hydrophobic tail on the inner layer.

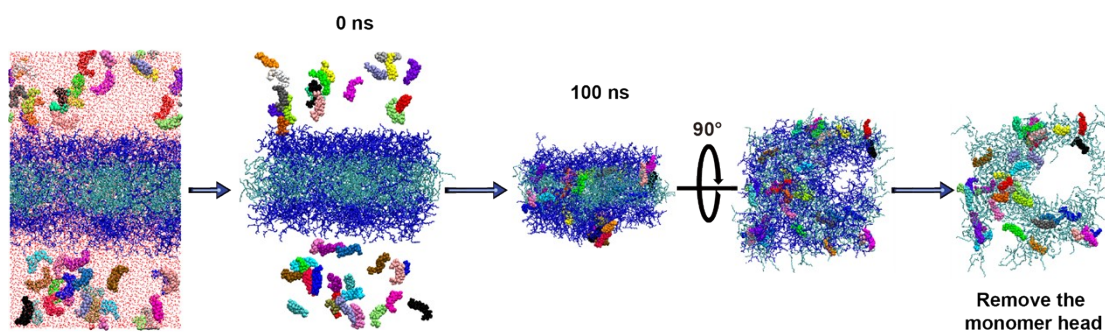


Figure S10. The Rh₂ molecules spontaneously integrate into the bilayer membrane created by dendritic macromolecular monomers, with Rh₂ primarily integrating into the hydrophobic region of the dendritic macromolecular monomers.

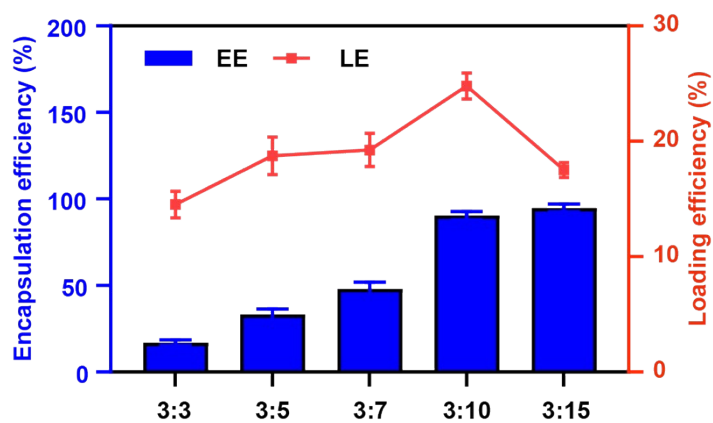
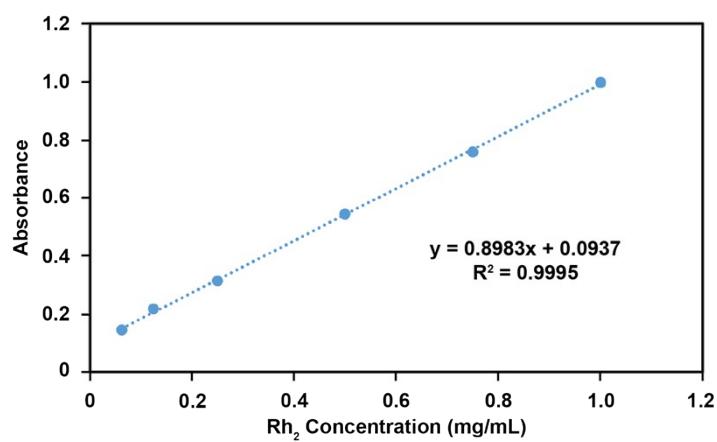


Figure S11. Standard curve constructed using Rh₂ methanol solutions of different concentrations. Drug loading content and efficiency are related to the ratio of Rh₂ to Lipo (n = 3).

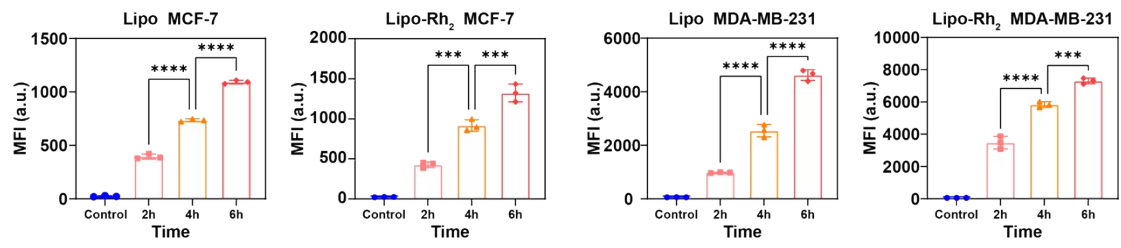


Figure S12. Statistical analysis of mean fluorescence intensity by flow cytometry, n=3.

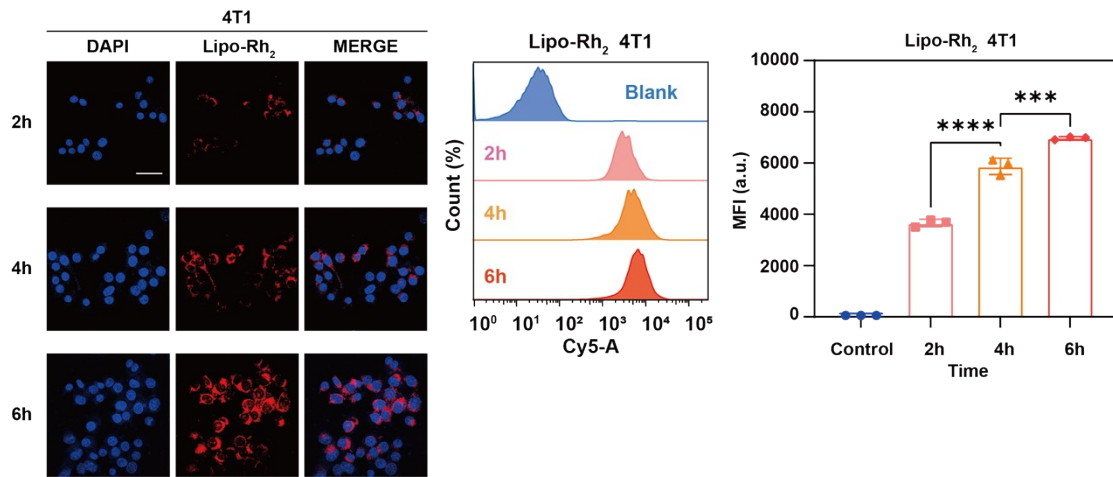


Figure S13. 4T1 cell uptake of Lipo-Rh₂ (scale bar 100 μ m) and verified cell uptake of Lipo-Rh₂ by flow cytometry.

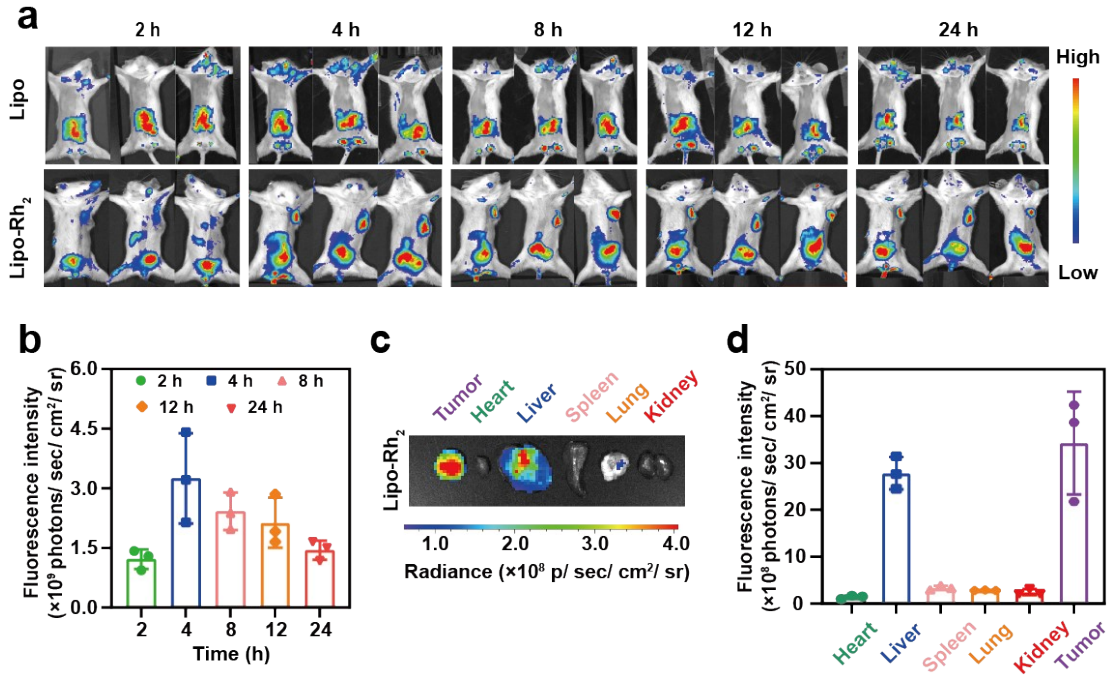


Figure S14. (a) Distribution map depicting the presence of Cy5-labeled Lipo and Lipo-Rh₂ bionic liposome in mice 24 hours post-administration. (b) Statistical analysis of the fluorescence intensity of Cy5-labeled Lipo-Rh₂ at time points after administration. (c) Harvested tumors and organs for fluorescence imaging 24 hours post-treatment. (d) Quantitative analysis of fluorescence intensity in tumors and organs. Data are expressed as the mean \pm SD, $n = 3$. Student's t tests were performed, $*P < 0.05$, $**P < 0.01$, $***P < 0.001$, $****P < 0.0001$.

Pharmacokinetic parameters							
IV Dose	1	mg/kg					
PK parameters	Unit	Rat 1	Rat 2	Rat 3	Mean	SD	CV(%)
Cl _{obs}	ml/min/kg	5.30	4.97	5.75	5.34	0.39	7.32
T _{1/2}	h	2.53	2.56	2.79	2.63	0.14	5.41
C ₀	µg/mL	24.63	29.24	24.08	25.98	2.83	10.91
AUC _{last}	h.µg/mL	3.09	3.32	2.87	3.09	0.23	7.36
AUC _{INF_obs}	h.µg/mL	3.14	3.35	2.90	3.13	0.23	7.26
AUC _{%Extrap_obs}	%	1.57	0.89	1.07	1.18	0.35	30.02
MRT _{INF_obs}	h	0.45	0.33	0.39	0.39	0.06	14.64
AUC _{last_D}	h.kg.µg/mL/mg	3.09	3.32	2.87	3.09	0.23	7.36
V _{ss_obs}	L/kg	0.14	0.10	0.13	0.13	0.02	18.05

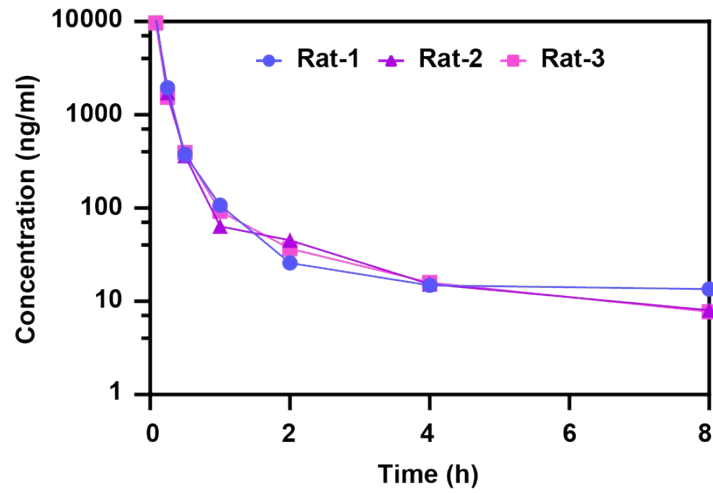


Figure S15. Pharmacokinetics of the bionic liposome Lipo-Rh₂ (SD rats, n = 3).

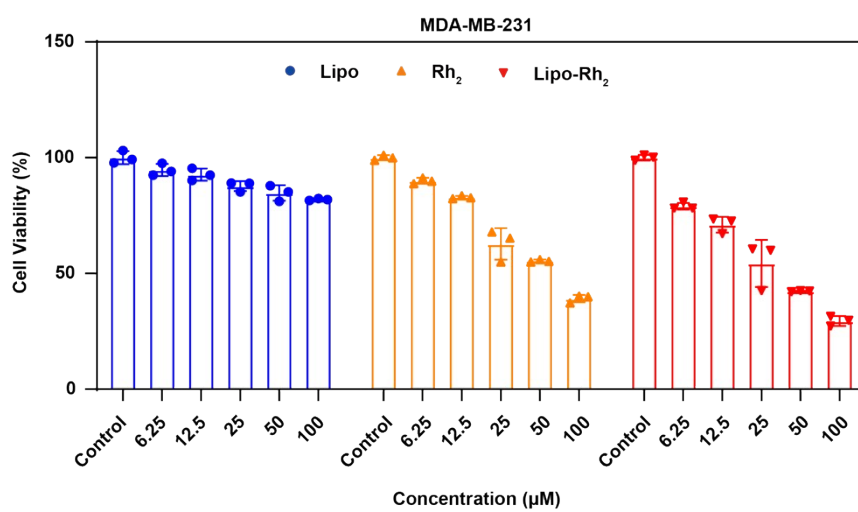


Figure S16. The effects of Lipo group, Rh₂ group, and Lipo-Rh₂ group on the cell viability of metastatic tumor cells MDA-MB-231, n =3.

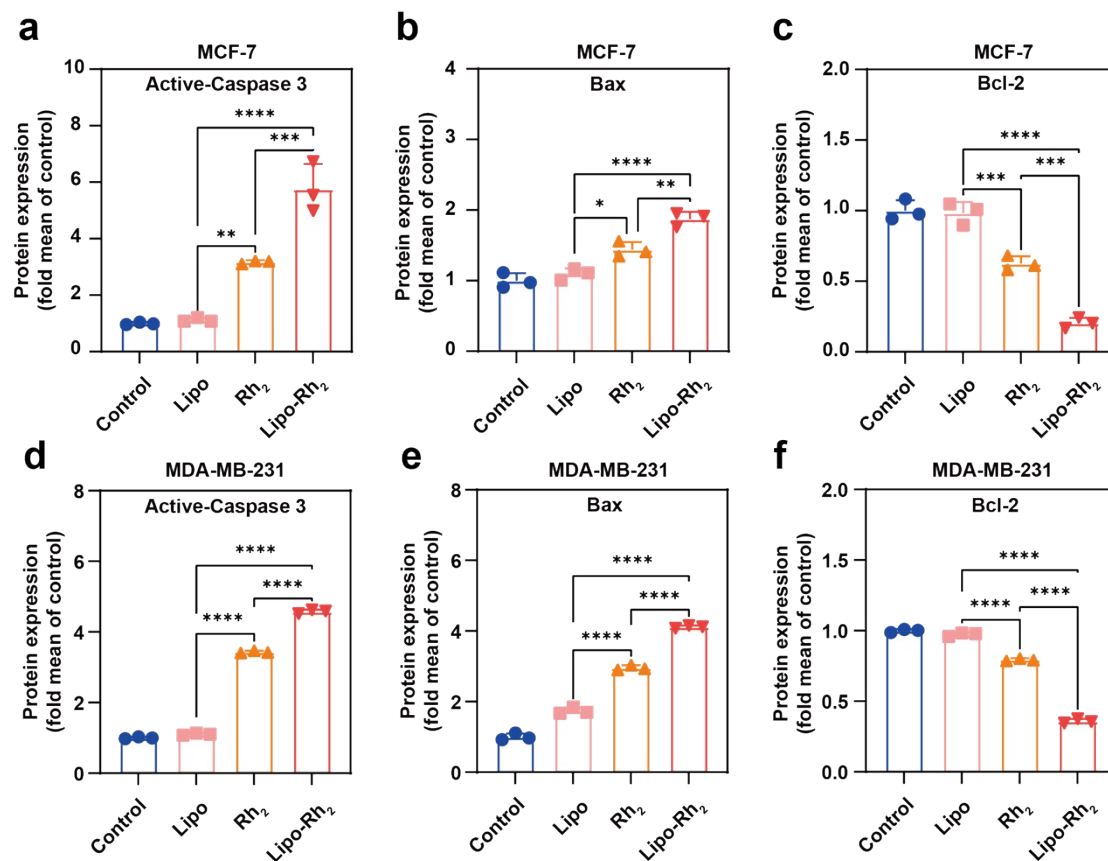


Figure S17. Statistical charts of tumor proliferation Western blot experiments for the MDA-MB-231 and MCF-7 cell lines, n = 3 (Corresponding to the Western blot experiment results in **Figure 2**).

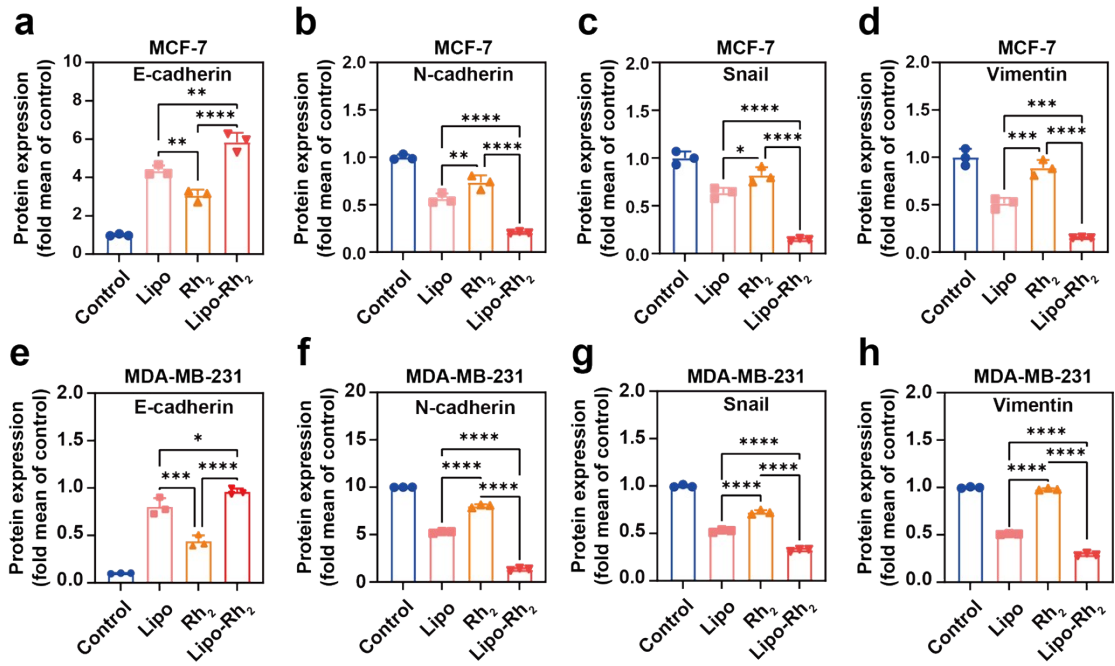


Figure S18. Statistical charts of tumor metastasis Western blot experiments for the MDA-MB-231 and MCF-7 cell lines, $n = 3$ (Corresponding to the Western blot experiment results in **Figure 3**).

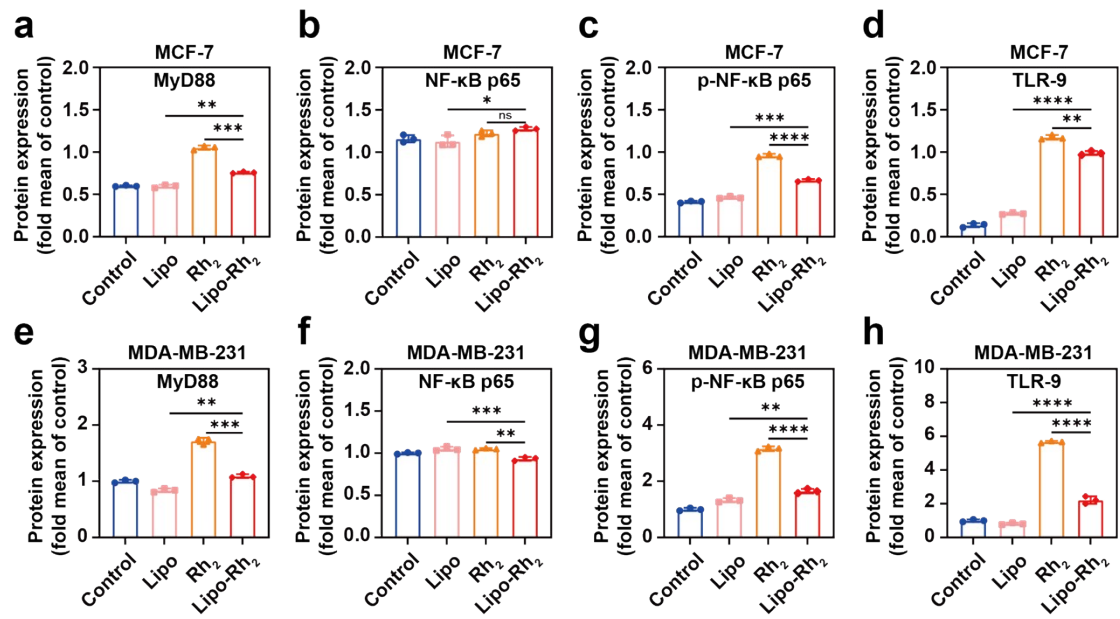


Figure S19. Lipo-Rh₂ inhibits the MyD88/NF-κB pathway as shown in the Western blot experiment statistical graph, n = 3 (Corresponding to the Western blot experiment results in **Figure 3**).

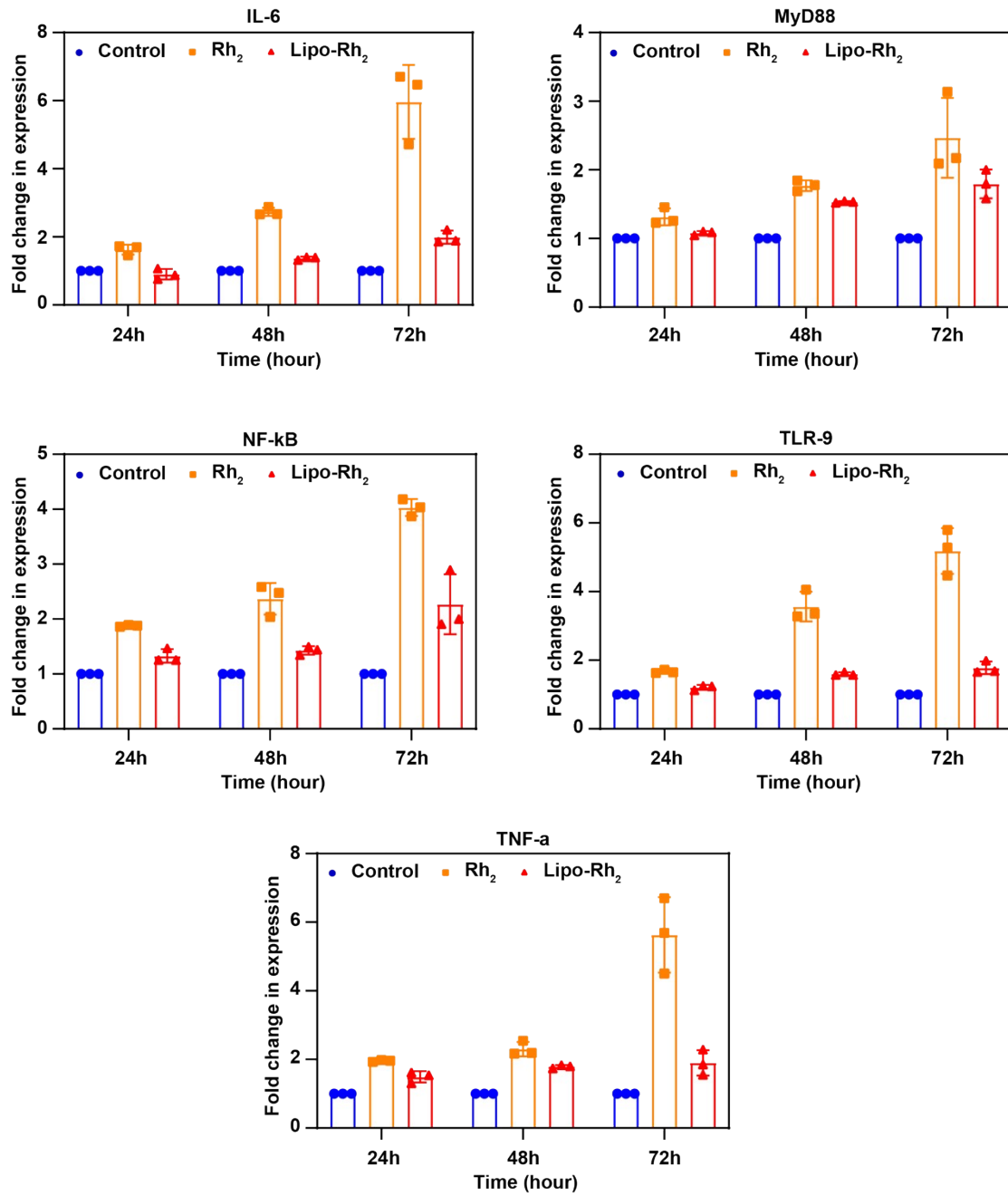


Figure S20. Fluorescent quantitative PCR analysis of the MyD88/NF-κB pathway, n = 3.

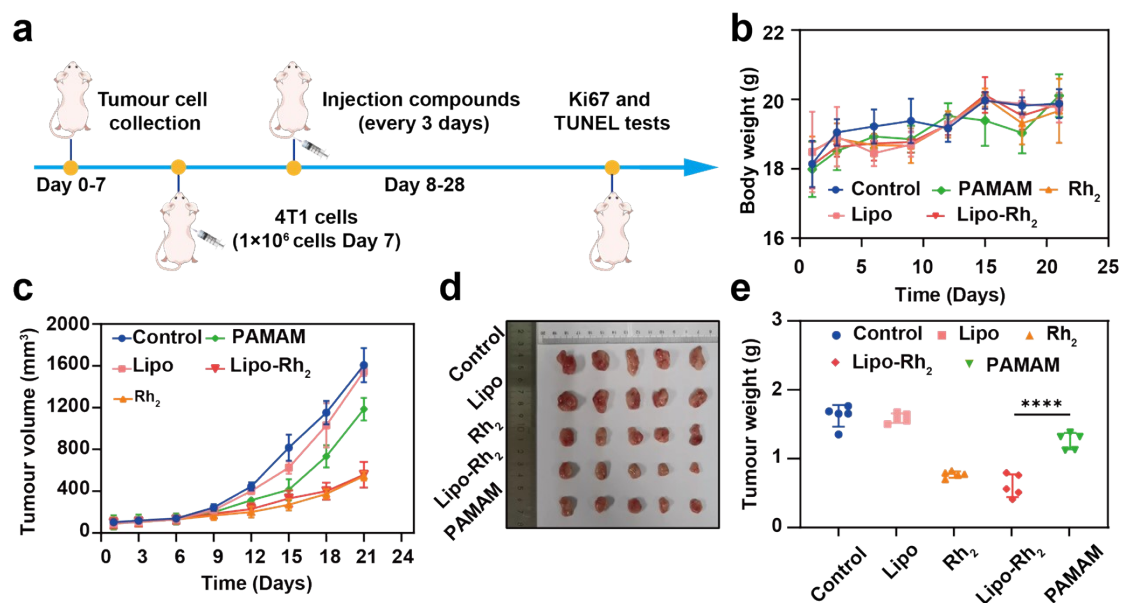


Figure S21. *In vivo* anti-tumor effects of lipo-Rh₂ bionic liposomes in a mouse subcutaneous tumor model. (a) Schematic diagram of the antitumor treatment process in mice. (b) Changes in mouse body weight throughout the experiment. (c) Changes in tumor volume in mice throughout the experiment. (d, e) Photographs of dissected tumors and tumor weight maps on the 21st day. Data are expressed as the mean \pm SD, $n = 5$. Student's *t* tests were performed, * $P < 0.05$, ** $P < 0.01$, *** $P < 0.001$, **** $P < 0.0001$.

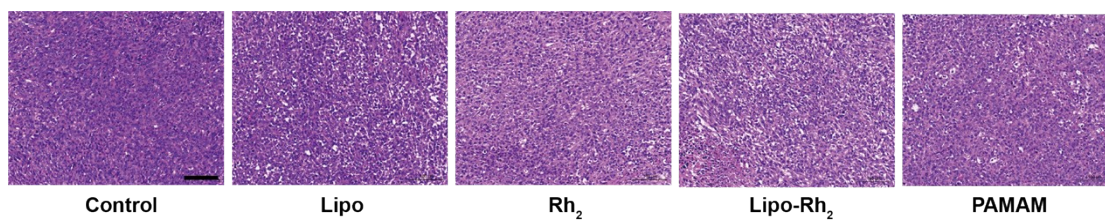


Figure S22. H&E diagrams of tumor tissues for each drug group (Scale bar 100 μm).

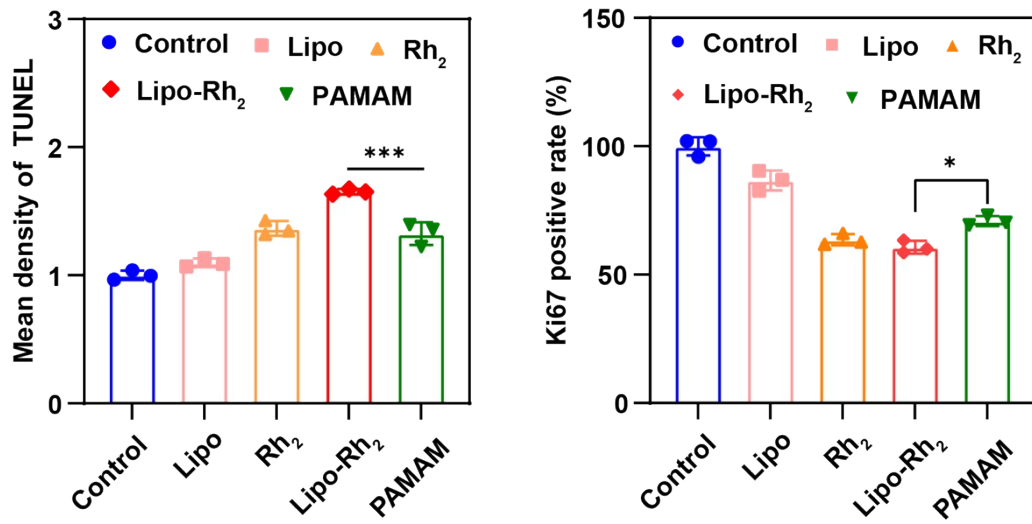


Figure S23. Statistical plots of data for TUNEL and Ki, n = 3.

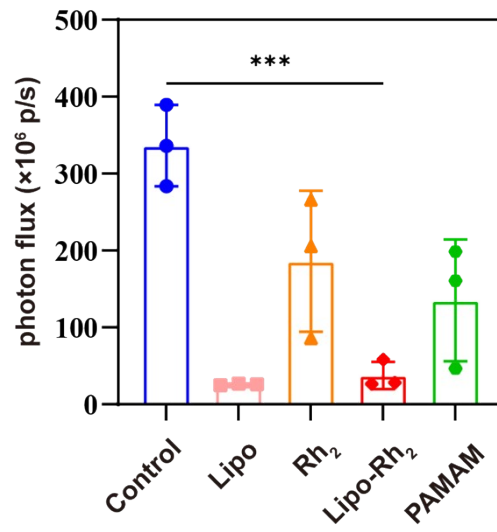


Figure S24. (a) Fluorescence intensity data statistics of mouse isolated lung, n = 3.

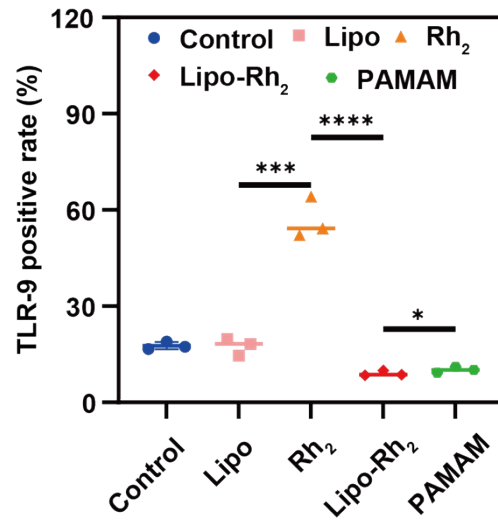


Figure S25. Immunohistochemical staining results of TLR-9, n = 3.

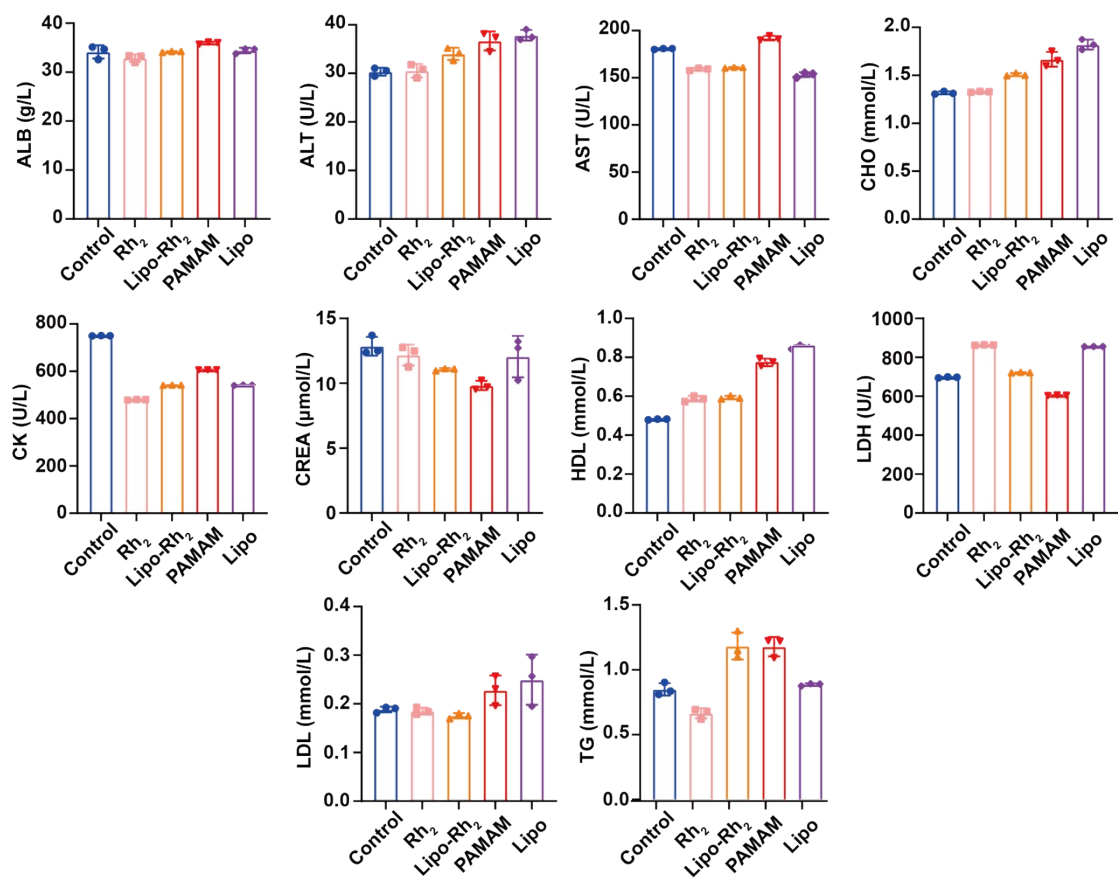


Figure S26. Biochemical testing of blood to assess the toxicity of various drugs on major organs (BALB/c mice, n = 3).

Table S1. Human primer sequences used for qPCR.

Primer name	Primer sequence (5' to 3')
hTLR9_F	CCA CCC TGG AAG AGC TAA ACC
hTLR9_R	GCC GTC CAT GAA TAG GAA GC
hIL-6_F	TCC ACA AGC GCC TTC GGT CCA
hIL-6_R	AGG GCT GAG ATG CCG TCG AGG A
hTNF-alpha_F	CCT GTG AGG AGG ACG AAC AT
hTNF-alpha_R	GGT TGA GGG TGT CTG AAG GA
hMYD88_F	CTC CTC CAC ATC CTC CCT TC
hMYD88_R	CGC ACG TTC AAG AAC AGA GA
hNFkB p50_F	TGGACAGCAAATCCGCCCTG
hNFkB p50_R	TGTTGTAATGAGTCGTCATCCT
hActin_F	ACC AAC TGG GAC GAC ATG GA
hActin_R	CCA GAG GCG TAC AGG GAT AG
NF-kB-F	GCAACTCTGTCCTGCACCTA
NF-kB-R	CTGCTCCTGAGCGTTGACTT